

© 2020 IEEE. Personal use of this material is permitted. Permission from IEEE must be obtained for all other uses, in any current or future media, including reprinting/republishing this material for advertising or promotional purposes, creating new collective works, for resale or redistribution to servers or lists, or reuse of any copyrighted component of this work in other works.

A Crown Quantization-Based Approach to Tree-Species Classification Using High-Density Airborne Laser Scanning Data

This paper appears in: IEEE Transactions on Geoscience and Remote Sensing (Early Access)

Date of Publication: 10 August 2020

Author(s): Aravind Harikumar, Claudia Paris, Francesca Bovolo, Lorenzo Bruzzone

Volume:

Page(s): 1 – 10

DOI: [10.1109/TGRS.2020.3012343](https://doi.org/10.1109/TGRS.2020.3012343)

A Crown Quantization Based Approach to Tree-Species Classification using High Density Airborne Laser Scanning Data

Aravind Harikumar, *Member, IEEE*, Claudia Paris, *Member, IEEE*, Francesca Bovolo, *Senior Member, IEEE*, and Lorenzo Bruzzone, *Fellow, IEEE*

Abstract—Crown features derived from high density Airborne Laser Scanning (ALS) data have proven to be effective for forest species classification at the individual tree level. Most of the general state-of-the-art techniques rely on coarse-level crown features extracted from ALS data, and under-utilize both the spatial and the spectral information available in the point clouds. Moreover, they are designed on the expected properties of the specific analyzed forest. We present a novel species classification approach, based on quantization of the entire 3D tree crown into smaller Elementary Crown Volumes (ECVs), that effectively captures the spatial distribution of filled (i.e., stem, branch and foliage) and empty volumes of crowns. In the first step, a data-driven process dynamically tests and compares three quantization strategies to tailor the definition of the ECV to the forest type (e.g., conifer, deciduous forest). In the second step, for each ECV a histogram vector is made-up by features representing the LiDAR point-distribution and intensity to model the internal and the external local crown characteristics. Then, tree histogram feature vectors are obtained by stacking all the ECVs histogram feature vectors. Finally, classification is performed by a Support Vector Machines (SVM) classifier using the histogram intersection kernel. All experiments were performed on three high density (50 to 200 points/m²) ALS datasets of deciduous, conifer, and mixed (i.e., both deciduous and conifer) trees. The higher classification accuracy of the proposed method over the state-of-the-art (SoA) one proves its ability to better capture the crown characteristics of individual trees, including species-specific traits.

Index Terms—Airborne Laser Scanning (ALS), High Density LiDAR Data, Tree Species, Classification, Histogram Feature Vector, Remote Sensing.

I. INTRODUCTION

The knowledge of tree species is crucial to accurate biophysical parameter estimation, forest management, and ecosystem studies [1]. In particular, the species detail at the individual tree level is of great significance for any comprehensive mapping of forest parameters including tree height, crown cover, stem diameter and biomass [2], [3]. Remote sensing is an effective and valid tool to monitor wide-area forests, and it is fast replacing the costly field based inventories. A variety of optical remote sensing data based methods have been developed to address the problem of tree species classification. Whatsoever, optical sensors have minimal visibility on the sub-canopy layers, and hence only

canopy level spectral characteristics [4], structure [5] and phenology [6] of tree(s) are usually modeled to achieve species classification. Thus, employing optical data for species classification in multi-layered forests may lead to poor species classification results.

Airborne Laser Scanning (ALS) scanning is an increasingly popular remote sensing technique for forest inventory collection. ALS scanning uses the airborne platform positional information from the Differential Global Positioning System (DGPS) and the orientation information from the Inertial Navigation System (INS) to assign accurate Three Dimensional (3D) geographic coordinates to the recorded laser signal intensities. ALS systems with single-return detection capability and low scanning frequency produce low density point clouds, and hence are suitable for species studies at the area level [7]. However, modern multi-return ALS scanners capture high density points cloud that encapsulates detailed crown structural details of tree(s) including stem, branch and foliage. For example, Leica ALS80 scanner has the capability to capture more than 50 points m² from a flying altitude of 1 km and with a speed of 100 km/hr. A denser point cloud also allows a better 3D delineation of individual tree crowns [8], and this nurtured the development of automatic individual tree level methods for species classification. Many individual tree crown delineation methods are based on 2D segmentation of the Digital Surface Model [9], and on 3D point cloud clustering [10], normalized cuts segmentation [11], graph based technique [12] and local re-projection of data points [13].

Species classification using ALS data is largely performed by modeling the differences in structural and or spectral characteristics of tree crowns [14], [15]. In particular, crown structural features are more reliably used over intensity ones due to the limited amount of spectral information in ALS, except for the case of multi-/hyper- spectral Light Detection and Ranging (LiDAR) data. Statistical features that model the point distribution within the crown provide details of the abstract/high-level characteristics of the tree. These features are successfully used in classification of tree species having considerable differences in foliage distribution characteristics along the crown height profile. Orka et al. [16] used statistical features representing both spatial and spectral crown characteristics from high density discrete-return LiDAR data to distinguish between conifer and deciduous trees. Based on the assumption that 3D crown shape varies for different species,

Aravind Harikumar, Claudia Paris and Lorenzo Bruzzone are with the Department of Information Engineering and Computer Science, Trento, Italy.

Aravind Harikumar and Francesca Bovolo E-mail: (see bovolo@fbk.eu) are with the Fondazione Bruno Kessler, Trento, Italy.

Manuscript received March 18, 2020

methods that model the tree crowns using paraboloid [17] and alpha shape [18] are also proposed. Although these approaches perform well for classifying trees belonging to different genera (i.e., that show considerable difference in crown shape), the performance is often suboptimal for classification of species that fall within the same genera. This motivated several authors to propose methods to extract the local crown structural characteristics. For example, Ko et al. [19] proposed a merge-and-split algorithm to model the branching structure within a crown, which allowed an automatic delineation of internal branch clusters followed by branch-level feature extraction. However, in addition to being largely affected by variance in point density, the method has a reduced accuracy for trees with increased branch complexity. Alternatively, Harikumar et al. [20] jointly used the branch level and overall crown features to perform species classification of four dominant European conifer species (Norway Spruce, European Larch, Swiss Pine, and Silver Fir), based on prior knowledge of conifer structure, they achieved an improved species classification accuracy over the state-of-the-art. Despite being costly in terms of money and computation, attempts were made to improve the species classification by supplementing the 3D structural information in LiDAR data with 2D optical and infrared data [21]. Many studies [22], [23] proposed to exploit the laser intensity together with the spatial data to perform species classification, and stress on the need for range normalization. However, highly rugged forest canopy results in range normalization ambiguities which distort the intensity data. Blomley et al. [24], performed tree species classification using features derived from projecting data to a vertical image plane that spins around the stem-axis and proved to be useful for drawing key crown structural traits. Although the method is robust to possible crown asymmetry, it fails to maximally exploit the 3D information provided by the LiDAR data.

From this literature overview, it turned out that, features designed for species classification are primarily: a) extracted at coarse scales resulting in under-exploitation of the both the structural and the spectral information in high density ALS data, and b) designed on prior expectations on the forest characteristics including species and sensor characteristics [24]. Moreover, current research on tree species classification mainly focuses on the extraction of feature parameters tailored to the peculiar classification problem, whereas little has been done to propose a data-driven approach able to handle heterogeneous forest classification problems [1]. Hence, there is a need to develop a species and forest independent approach that automatically derives optimal features by maximally exploiting the local crown information. We propose an approach to tree species classification in ALS point clouds, that divides the crown volume in sub-volumes referred to as the Elementary Crown Volumes (ECVs). The division process is referred to as quantization. The quantization is conducted under the assumptions that: a) trees have a central stem surrounded by branches growing away from the stem, and b) local branch structure, foliage density and laser reflectance vary over the crown in a unique and species-dependent way (thus points in ECVs are used to extract representative features). The proposed species classification

approach: a) automatically detects the optimal 3D quantization strategy without requiring any prior knowledge on the forest type and or species, b) mitigates the effect of point density variance within the crown, c) defines tree histogram feature vectors to capture efficiently the complex crown structures, d) extensively exploits the information provided by the 3D LiDAR point cloud by performing a fine/localized analysis of crown point cloud, and e) performs species classification by using a Support Vector Machine Classifier (SVM) with histogram kernel. The potential of the proposed method lies in its capability to capture the local variation in crown characteristics, by means of features extracted from point cloud in individual ECVs, and to perform an accurate supervised classification of different tree species.

The rest of the manuscript is structured as follows. Section II presents the proposed method to tree species classification. The details about the dataset, the experiments, and the results are illustrated in Section III. Finally, Section IV concludes the paper and presents some prospective future developments.

II. PROPOSED TREE SPECIES CLASSIFICATION APPROACH

The workflow of the proposed method is shown in Figure 1. In the considered implementation, the individual tree crown delineation is performed directly in the 3D point cloud space as proposed in [13]. However, any other method that allows an accurate 3D individual crown delineation can be employed [8]. For each segmented tree point cloud, the proposed method performs the ECV quantization of the crown by testing three strategies including, a) angular, b) radial and c) hybrid quantization. For each quantization strategy, a set of features are extracted representing the LiDAR point-distribution, the internal and the external crown structure [25], [26]. This condition allows us to adaptively determine the best set of ALS features for different classification problems. The tree histogram feature vector is calculated by stacking all the ECVs histogram feature vectors. Finally, the species classification is performed by using a SVM with histogram kernel. It is worth noting that the proposed method directly operates in the 3D point cloud space.

Figure 2 shows the cylindrical model used to define the bounding volume of the 3D segmented tree point cloud. Let p_t and g_t be the highest point of the segmented tree point cloud and its projection onto the ground (i.e., XY plane), respectively. The line L_t connecting p_t and g_t represents the vertical axis of the tree, i.e., the tree stem. The maximum radius r_t of the tree crown t_i is the shortest distance between the L_t , and the farthest LiDAR point from it, i.e., p_t . The maximum height h_t of the tree crown is the highest point in the tree point cloud. These parameters define a cylindrical volume that contains the entire tree point cloud having angular $\alpha \in [0, 2\pi]$, radial $\rho \in [0, r_t]$ and height $\zeta \in [0, h_t]$ coordinates, where $t \in (1, T)$ and T is the total number of trees.

A. Elementary Crown Volume Quantization

By taking advantage of the cylindrical model representation of the crown, the proposed method performs a 3D quantization

of the volume spanned by the cylinder along the α , the ρ and the ζ dimensions to generate sub-volumes, i.e., the ECVs. The shape and size of the ECVs determine the local section of the crown leading to unique crown perspectives/details. For this reason, the proposed method tests and compares three crown Quantization Strategies (QS) which include: a) angular, b) radial and c) hybrid options.

The *angular quantization* strategy, referred to as QS_{α} , simultaneously quantizes the cylindrical volume along the α and ζ dimensions into α_N and ζ_N quantization steps, respectively (Figure 3a). With such quantization, the shape of the resulting ECV is a cylindrical sector. Spatial and spectral features derived from the set of these ECVs represent the structure of branch/foliage and intensity distribution along the α dimension.

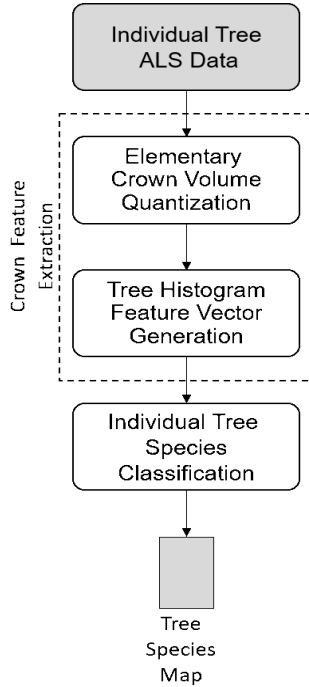


Fig. 1: Workflow of the proposed crown quantization based individual tree species classification method.

The *radial quantization* strategy, referred to as QS_{ρ} , simultaneously quantizes the cylindrical volume along the ρ and ζ dimensions into ρ_N and ζ_N quantization steps, respectively (Figure 3b). Here, each ECV has a cylindrical annular shape, and models the structural variations along the radial direction of the crown. In particular, the features derived from this set of ECVs represent the branch/foliage structure and intensity distribution along the ρ dimension.

The *hybrid quantization* strategy, referred to as $QS_{\alpha\rho}$, simultaneously quantizes the cylindrical space in α_N angular, ρ_N radial and ζ_N quantization steps along the α , ρ and the ζ dimensions, respectively (Figure 3c). The shape of the ECV is a cylindrical annular sector which allows us to model complex structural variations within the crown. Here, the branch/foliage structure and intensity distribution along both the α and the ρ dimensions are represented by the features derived from the ECVs.

The proper representation of the trees requires the definition of quantization steps to model the complex structural variations within the crown. Here, we propose a tree-independent strategy such that the cylindrical dimensions r_t and or h_t along the ρ and ζ dimensions are fixed (i.e., the radius and the height of the cylinder are the same for every tree). In this context, the quantization step along the angular direction α is

$$\delta_{\alpha} = \frac{2\pi}{\alpha_N}; \quad (1)$$

the one along the radial direction ρ is,

$$\delta_{\rho} = \frac{r_{max}}{\rho_N}; \quad (2)$$

and the one along the height direction ζ is,

$$\delta_{\zeta} = \frac{h_{max}}{\zeta_N}; \quad (3)$$

where r_{max} and h_{max} represent the maximum radius and height within the considered set of trees, respectively. Enforcing a fixed cylindrical dimension for every tree allows the proposed method to model data-free volume between tree crown and the enclosing cylinder. Hence, ECVs with at least one point define the filled crown volume, while those without any point define the void crown volume (mostly between the crown surface and the cylindrical boundaries). This void volume differs in size and spread, with species. In particular, the difference in spread of data-free volume within and beyond the crown is useful in indirectly modeling: a) the internal distribution of the branches and foliage, b) the external crown geometric characteristics, and c) the overall crown span within the cylindrical volume.

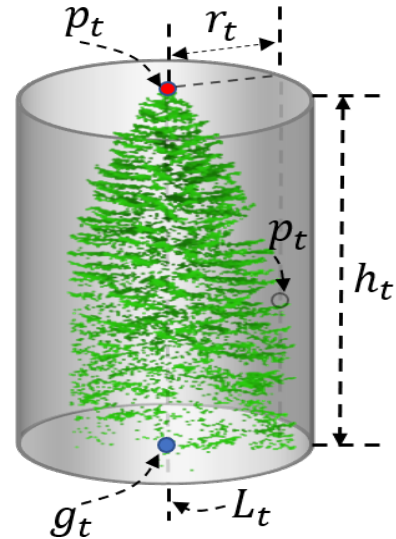


Fig. 2: Cylindrical model used to define the bounding volume of the segmented tree point clouds. p_t , g_t and r_t are the highest point of the segmented tree point cloud, the projection of p_t onto the ground, and the radius of the cylinder, respectively. L_t is the cylinder axis assimilated to the tree-stem axis.

If we assume V to be the number of ECVs generated per tree, which is equal to $\alpha_N \cdot \zeta_N$, $\rho_N \cdot \zeta_N$, and $\alpha_N \cdot \rho_N \cdot \zeta_N$ for the angular, radial, hybrid quantization strategies, respectively, the

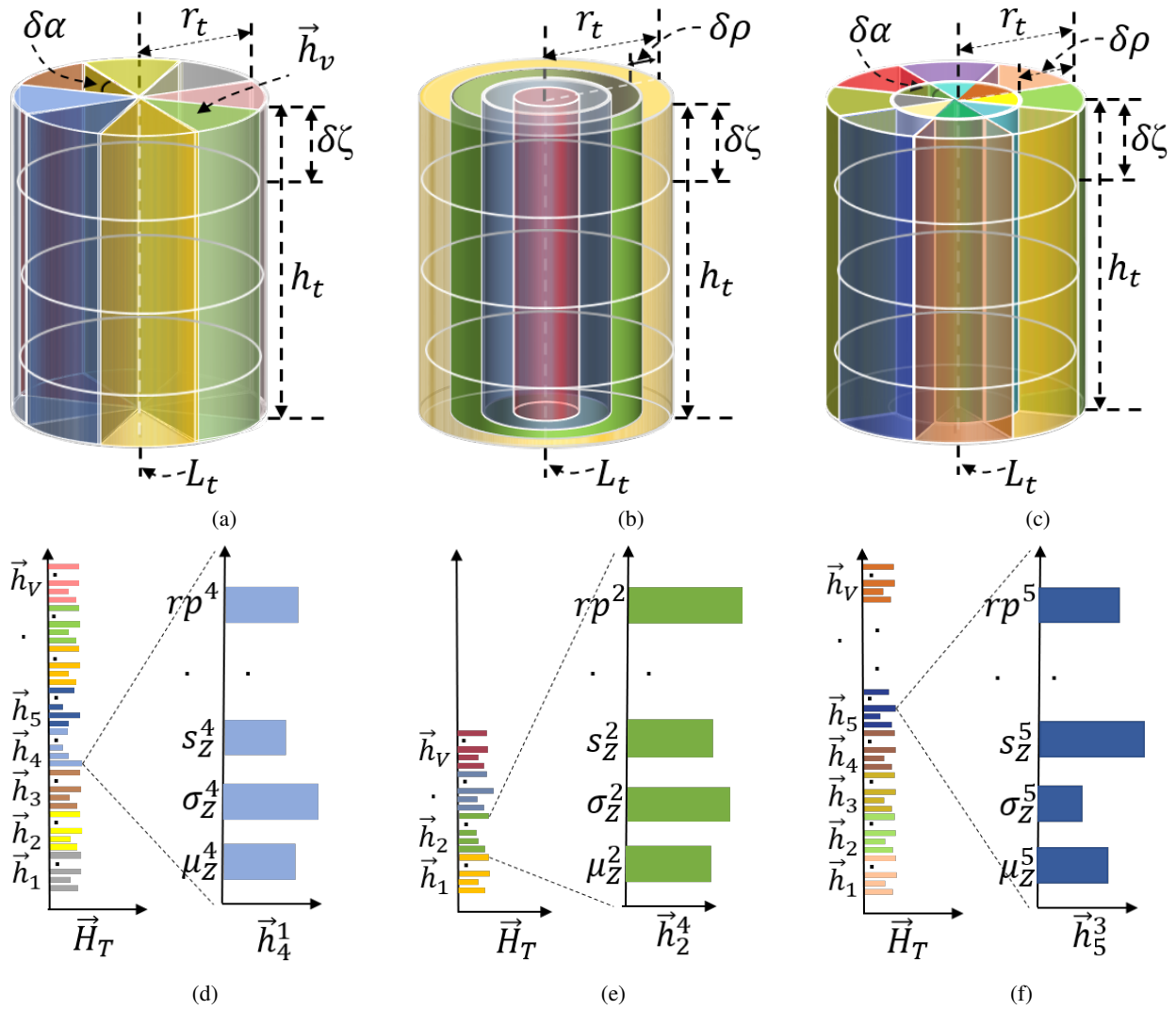


Fig. 3: The ECVs obtained considering the: (a) angular QS_α (b), radial QS_ρ (c) and hybrid $QS_{\alpha\rho}$ quantization strategy. For each quantization strategy, the obtained ECVs are highlighted in different colors. The tree histogram feature vector \vec{H}_T obtained by stacking all the ECVs histogram feature vectors extracted from its crown \vec{h}_v , $v \in [1, V]$ are reported for the: (c) angular QS_α , (d) radial QS_ρ (e) and hybrid $QS_{\alpha\rho}$ quantization strategy.

v^{th} quantization volume ECV $_v$, $v \in [1, V]$ encloses a unique set of LiDAR points which represents the local crown structure within the sub-volume.

B. Generation of the Tree Histogram Feature Vector

For each ECV, the proposed method generates an histogram feature vector considering the set of standard features reported in Table I, [1]. The f_Z , f_D and f_I feature sets are derived from height, positional and intensity attributes of points in each ECV, where $f = [\mu, \sigma, s, k]$ are the mean, the standard deviation, the skewness and the kurtosis features, respectively. Together with the statistical distribution of the input features, we model the geometric shape of local crown components based on the 3D spread of points in each ECV, i.e., rp . This feature models the distribution of local linear structure within the crown. Thus, the root mean squared error corresponding to regression fitting a plane P_R on ECV points will be minimum in the presence of linear structures such as stem and branches,

while the error will be relatively higher for volumes containing mostly foliage. The v^{th} ECV histogram feature vector $\vec{h}_v = [\mu_Z^v, \sigma_Z^v, \dots, rp^v]$ is derived from the attributes (i.e., position and intensity) of the LiDAR points that are enclosed in the considered ECV to model the local crown structure. The tree histogram feature vector \vec{H}_T is obtained by stacking all the ECVs histogram feature vectors extracted from its crown, i.e., $\vec{H}_T = [\vec{h}_1, \vec{h}_2, \dots, \vec{h}_V]$ (Figure 3d, 3e and 3f).

Due to laser obstruction by crowns themselves, the number of laser points tends to decrease: a) from the tree top to the bottom, and b) from the outer to the inner region of the crown. Thus, the features have to be normalized before performing the classification step. The normalization strategy aims to mitigate the effect of point density variation under the assumption that the scan-density is comparable in ECVs which are equidistant from L_t . To this end, a global normalization is performed separately for each feature type in \vec{h}_v (i.e., μ, σ, s, k and rp) for all the ECV histogram feature vectors \vec{h}_v , $v \in [1, V]$ belonging to

to the crown, as follows,

$$\vec{H}_{T_n^i} = \frac{[\vec{h}_1^i, \vec{h}_2^i, \dots, \vec{h}_V^i]}{\max_{v=1, \dots, V} (\vec{h}_v^i)} \quad (4)$$

C. Individual Tree Species Classification

The normalized tree histogram feature vector \vec{H}_{T_n} encompasses the entire crown structural information. To accurately perform the classification of the individual tree species, we considered an SVM classifier with histogram intersection kernel $K_{hist}(\cdot)$ [27]. This kernel performs better compared to other nonlinear kernels on challenging classification problems having high dimensional feature spaces since it: a) assigns maximum weights to key features, b) optimizes computational performance despite a large number of features, and c) generalizes well through efficiently modeling the sparsity of data. Moreover, the $K_{hist}(\cdot)$ kernel is a positive definite parameter-free kernel for histogram-based features, such as the ones defined in Sec. II-B. Accordingly, even though the proposed method may generate high-dimensional tree feature vector when considering small quantization steps, due to the high generalization capability of SVM with the $K_{hist}(\vec{H}_{T_n}^p, \vec{H}_{T_n}^j) = \sum_{p,j=1}^{v_l} \min(\vec{H}_{T_n}^p, \vec{H}_{T_n}^j)$ kernel with $\vec{H}_{T_n}^p \geq 0, \vec{H}_{T_n}^j \geq 0$, the classification results do not suffer from the curse of dimensionality (i.e., the classification accuracy does not decrease when increasing the number of features beyond a given threshold). The objective function of the SVM with histogram intersection kernel has the following dual form,

$$\begin{aligned} & \underset{a_p \in [0, C]}{\text{maximize}} && \sum_{p=1}^{v_l} a_p - \frac{1}{2} \sum_{p=1}^{v_l} \sum_{j=1}^{v_l} a_p a_j y_p y_j K_{hist}(\vec{H}_{T_n}^p, \vec{H}_{T_n}^j) \\ & \text{subject to} && \sum_{p=1}^{v_l} a_p y_p = 0, \text{ and } 0 \leq a_p \leq C \text{ for } \forall p. \end{aligned} \quad (5)$$

Here, \vec{H}_{T_n} and $y \in \{-1, 1\}$ are the data samples and the corresponding labels, respectively. The regularization parameter is denoted as C , and v_l is the total number of samples. The support vectors to derive optimal hyperplane parameters can be estimated using quadratic programming methods by maximizing (5).

III. EXPERIMENTS AND RESULTS

A. Dataset Description

The considered forest is located in a mountain area in the municipality of Pellizzano, at about 40 km northwest of the city of Trento in Italy. The area extends approximately 3200 Ha and the altitude ranges from 900 to 2000 meters above sea level. The forest is mainly dominated by conifer species such as Norway Spruce (*Picea abies*), European Larch (*Larix decidua*), Swiss Pine (*Pinus cembra*), Silver Fir (*Abies alba*), and a small presence of deciduous trees such as Silver Birch (*Betula pendula*) and Rowan (*Sorbus aucuparia*), hereafter referred as AR, EL, SP, SF, SB and RO, respectively.

TABLE II: Statistics of the structural properties of the considered tree crowns.

Tree Species	Number of Trees	Tree height (m)			Crown width (m)		
		Max	Min	Mean	Max	Min	Mean
NS	50	43.6	16.3	30.8	6.5	2.4	4.5
EL	50	40.7	12.1	27.3	9.0	2.8	5.5
SP	50	20.6	8.0	14.2	5.4	1.2	3.3
SF	50	39.5	15.7	30.6	6.2	2.8	4.7
SB	50	19.4	6.5	11.5	7.0	2.1	3.6
RO	50	29.5	5.7	10.5	11.7	2.4	4.3

The ALS data were acquired between 7th and 9th September 2012 using a Riegl LMSQ680i sensor operated at a scanning frequency of 400 KHz from an airborne platform flown at an altitude of 660 m with a speed of 100 Km/hr allowing acquisition of 10 - 50 points/m². The variation in point density is a result of altitude variation from 900 to 2000 m and the effect of scan direction. The flight was repeated several times to obtain very high density cloud of 50 to 200 points/m². This results in an average point density of 12000 points per tree. All experiments were conducted on a set of 300 trees, with 50 trees per species. Table II shows the tree height and maximum crown width statistics of the tree samples. The ALS point cloud representations for the six tree species and their internal crown structures are illustrated in Figure 4 and Figure 5, respectively. As one can notice, the LiDAR point distribution provides an explicit characterization of tree crown geometries. While, the range-normalized intensity attribute [28] is used to derive spectral characteristics of crown. However, to accurately capture the distinctive properties of each tree species, a proper quantization is necessary to decompose the structure of the tree.

B. Experimental Setup

To validate the proposed method we evaluate its capabilities in selecting the best quantization strategy (among the proposed ones) and the goodness of the proposed set of structural features in terms of classification accuracy. The available data are divided to simulate three forest scenarios with different species and variable complexity: (a) deciduous, (b) conifer and (c) mixed. The first scenario represents a deciduous forest and includes two broad-leaves species. They show similar behaviours in terms of crown shape and height (Figure 4e and 4f). Hence, even though broad-leaves are usually separable by standard geometric features, the similarity in external crown properties leads to poor classification accuracy with standard methods. The second scenario includes four tree species from the conifer class. The four species show minor differences in crown external features, and major differences in the internal tree crown structure (i.e., the branch structure is one of the most peculiar feature to distinguish conifers) [20]. The third one is the most complex scenario of mixed forest, which requires data-driven approaches that can handle the traits that characterizes conifer and deciduous trees. Indeed, many of the established methods fail when dealing with heterogeneous forest stands [1]. The three scenarios allow to demonstrate that

TABLE I: Crown geometric features derived from each ECV. z_i , d_i and t_i are height, distance to respective ECV data-point centroid, and intensity of the point p_i . P_R is the regression fitted plane on the points within an ECV.

Group Id	Feature Id	Description	Equation
f_Z	μ_Z^v	Mean of the z_i values for all of the laser points n representing the v^{th} ECV.	$\frac{\sum z_{i=1}^n}{n}$
	σ_Z^v	Standard deviation of the z_i values for all of the laser points n representing the v^{th} ECV.	$\sqrt{\frac{\sum_{i=1}^n (z_i - \bar{z})^2}{n-1}}$
	s_Z^v	Skewness of the z_i values for all of the laser points n representing the v^{th} ECV.	$\frac{\sum_{i=1}^n (\frac{z_i - \bar{z}}{\sigma_Z^v})^3}{n}$
	k_Z^v	Kurtosis of the z_i values for all of the laser points representing the v^{th} ECV.	$\frac{\sum_{i=1}^n (\frac{z_i - \bar{z}}{\sigma_Z^v})^4}{n} - 3$
f_D	μ_D^v	Mean of the d_i values for all of the laser points n representing the v^{th} ECV.	$\frac{\sum d_{i=1}^n}{n}$
	σ_D^v	Standard deviation of the d_i values for all of the laser points n representing the v^{th} ECV.	$\sqrt{\frac{\sum_{i=1}^n (d_i - \bar{d})^2}{n-1}}$
	s_D^v	Skewness of the d_i values for all of the laser points n representing the v^{th} ECV.	$\frac{\sum_{i=1}^n (\frac{d_i - \bar{d}}{\sigma_D^v})^3}{n}$
	k_D^v	Kurtosis of the d_i values for all of the laser points representing the v^{th} ECV.	$\frac{\sum_{i=1}^n (\frac{d_i - \bar{d}}{\sigma_D^v})^4}{n} - 3$
f_I	μ_I^v	Mean of the t_i values for all of the laser points n representing the v^{th} ECV.	$\frac{\sum t_{i=1}^n}{n}$
	σ_I^v	Standard deviation of the t_i values for all of the laser points n representing the v^{th} ECV.	$\sqrt{\frac{\sum_{i=1}^n (t_i - \bar{t})^2}{n-1}}$
	s_I^v	Skewness of the t_i values for all of the laser points n representing the v^{th} ECV.	$\frac{\sum_{i=1}^n (\frac{t_i - \bar{t}}{\sigma_I^v})^3}{n}$
	k_I^v	Kurtosis of the t_i values for all of the laser points representing the v^{th} ECV.	$\frac{\sum_{i=1}^n (\frac{t_i - \bar{t}}{\sigma_I^v})^4}{n} - 3$
rp^v	Regression plane fit Root Mean Squared Error.		$\sqrt{\frac{\sum_{i=1}^n (p_i - P_R)^2}{n}}$

the proposed approach is able to deal with multiple kinds of forest and no prior knowledge on their composition is required.

For all the experiments, the reference data were split into training, validation and test data corresponding to 70%, 20% and 10% of the total number of trees. The training set is used to train the classifier and select the regularization parameter of the SVM by 5 fold cross-validation in steps of one decade in the range $[10^{-3}, 10^3]$. The test set is used to perform the independent assessment of the classification results. The optimal quantization strategy and parameters are selected in a classification-performance based sensitivity analysis, by selecting the strategy (among QS_{α} , QS_{ρ} , and $QS_{\alpha\rho}$) which gives the highest classification performance on the validation set. In detail, the optimal δ_{α} , δ_{ρ} and δ_{ζ} quantization steps are obtained by testing α_N in the range $[5, 180]$ with step of 5, ρ_N in the range $[1, 15]$ with step of 1, and ζ_N in the range $[5, 100]$ with step of 5. A larger number of steps is avoided since smaller ECVs would provide less meaningful features failing to capture the local structural information. The maximum width r_{max} and height h_{max} in the dataset are 11.7m and 43.6m, respectively.

Table IV reports the OA obtained on the validation set considering the three quantization strategies for the three forest types. While the Radial quantization performs best on the deciduous forest (i.e., an OA% of 94.2), the hybrid quantization is able to extract the best local crown structural features for the mixed forests (i.e., an OA% of 77.1). Similar results are obtained on the conifer forest for both radial and hybrid quantization (i.e., an OA% of 72.3). The optimal combinations of quantization parameters α_N , ρ_N and ζ_N are 8, 4, and 70 for both the conifer and the mixed forest, respectively, while for the deciduous the best α_N and ζ_N are 8 and 60, respectively. As expected the worst results are obtained with the angular quantization, where sub-volumes do not characterize the complex crown characteristics of the considered tree species (Figure 5). The results obtained with the angular strategy demonstrate the importance of having a proper tree crown quantization for an accurate classification. Thus, even though it is necessary to extract meaningful features from the physical view point, a proper quantization is fundamental to capture the local structural proprieties of the tree crowns.

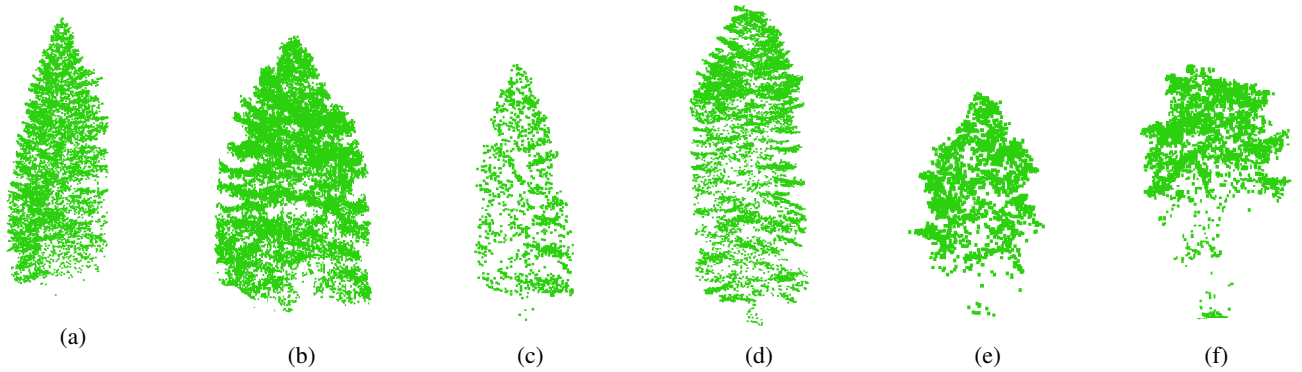


Fig. 4: Side view ALS data of the sample trees represented: (a) Norway Spruce (NS), (b) European Larch (EL), (c) Swiss Pine (SP), (d) Silver Fir (SF), (e) Silver Birch (SB) and (f) Rowan (RO).

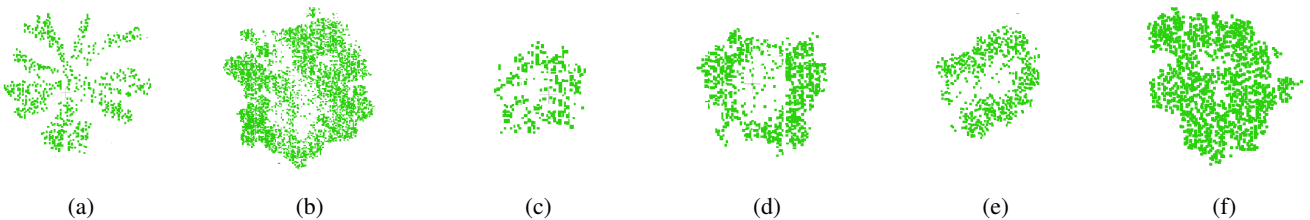


Fig. 5: Top view of ALS data (1m vertical slice) of the sample trees represented: (a) Norway Spruce (NS), (b) European Larch (EL), (c) Swiss Pine (SP), (d) Silver Fir (SF), (e) Silver Birch (SB) and (f) Rowan (RO).

C. Experiments, Results and Discussion

We assess the effectiveness of the proposed approach by comparing it with the state-of-the-art (SoA) method proposed in [1], where a comprehensive set of features are defined based on: a) spatial point distribution, b) return intensity distribution, c) internal crown structure, and d) external crown structure. The authors analyze the classification accuracy obtained by integrating the best features from different categories to avoid the curse of dimensionality phenomenon. Here, we used the optimal combination of features only (see Table III). The proposed method does not perform feature selection, instead. This is because of the effectiveness of the histogram intersection kernel in handling high-dimensional histogram-based features. For both the proposed and the SoA methods, the multi-class situation was handled using the one-against-one classification strategy with SVM. For the proposed method, the results reported are the ones obtained with the quantization strategy and parameters that achieve the highest classification accuracy on the validation set.

Table V, Table VI and Table VII show the Producers Accuracy (PA), User Accuracy (UA), and Fscore (F1) for the proposed and the SoA methods obtained on the test set for the deciduous, conifer and mixed forests, respectively. From the results one can notice that the proposed approach obtains high classification accuracy regardless of the forest type. Moreover, it sharply improves the results of the SoA method for all the scenarios by achieving an OA of 93.3%, 86.6% and 76.6% vs 56.6%, 61.6% and 52.2% for deciduous, conifer and mixed forest, respectively. This is due to the fact that the proposed approach: (i) extensively exploits the

local crown structural information in the ALS data, (ii) relies on feature parameters automatically tailored to the specific classification problem with no prior information on species. Although the deciduous scenario includes two species with similar crown properties, the proposed approach achieves the highest OA compared to the other classification tasks, with an F1% 0.93 for both SB and RO. The SoA approach results in poor classification metrics with an F1% of 0.55 and 0.58 for the SB and RO, respectively. Hence, the standard geometric features demonstrate to be insufficient in capturing the small differences of the internal and external structural properties which distinguish these two species. SoA method performs better in the conifer scenario rather than on the deciduous one. F1% ranges between 0.48 (for SP) and 0.82 (for SF). However, the proposed method performs better in average over all the species showing an F1% that ranges between 0.80 (for EL) and 0.93 (for SP). It is worth noting that conifers have similar external structural behaviours due to the general conical shape of their crown, yet not identical. This leads to a number of empty EQVs towards the top of the crown. The SVMs with histogram kernel properly captures and handles this property resulting in robust and accurate classification performance, whereas the standard features fail in doing so. As expected, for both the proposed and the SoA methods the most complex scenario is represented by the mixed forest containing both conifer and deciduous trees. While the maximum F1% achieved by the SoA approach is 0.57 (for SB), the proposed method obtains 0.90 (for NS). Moreover, despite the complexity, the proposed approach achieves a classification accuracy comparable to the ones obtained for the homogeneous forest types due to its

TABLE III: SoA features from [1]. Here I_n is the intensity of the n^{th} laser point, n is the the total number of data points representing the target tree. H_{G_i} is the height of the i^{th} grid. N_G is the number of vertical grids for a tree. A_{base} is the crown base area. L_s and L_{cs} are longest spread and cross-spread of tree crown, respectively.

Feature Id	Description	Equation
$f_{I_{0-20}}$	Mean of the intensity I_i values for the laser points lying within 0^{th} - 20^{th} percentile of tree height (from tree bottom)	$\bar{I}_{n_i=1: 0.0h_T \leq z_i < 0.2h_T}$
f_{cl}	Ratio between the height of the equivalent centers for the grids within each profile and the crown length (average for 8 profiles)	$\frac{\sum_8 (\sum_{i=1}^n H_{G_i} / n)}{8L_c}$
f_{stem}	Ratio between the number of the grids for the stem-related space and all of the grids for a tree (stem-related space: 1/3 tree height from bottom, 1/2 crown diameter)	$\sum \frac{N_{G_{down \& within 0.5 crown}}}{N_G}$
f_{ecd}	Equivalent crown diameter	$2\sqrt{A_{base}}$
f_{csr}	Ratio between L_s and L_{cs} .	$\frac{L_s}{L_{cs}}$
f_c	Mean height for all of the grids representing a tree.	$\sum_{i=1}^n (H_{G_i} / n)$

TABLE IV: Best Overall Accuracy (OA%) obtained on the validation set by testing the different quantization strategies and parameters on the deciduous, conifer, and mixed forest.

	Overall Accuracy (OA %)		
	Angular	Radial	Hybrid
	Quantization	Quantization	Quantization
Deciduous Forest	92.8	94.2	88.5
Conifer Forest	70.0	71.4	77.1
Mixed Forest	69.0	72.3	72.3

capability of dynamically selecting the optimal feature set and quantization strategy for considered classification task. Form the computational view point, the larger number of local features extracted from the crown makes the proposed approach slightly more demanding compared to the SoA. However, the proposed approach can perform the classification of each tree separately and in parallel, thus it is possible to strongly reduce the computational effort at large scale. Finally, the proposed method does not require any hand-crafted feature selection based on prior knowledge of the considered forest area. This condition is extremely important to deal with large forests characterized by heterogeneous properties.

TABLE V: Classifications performance obtained on the test set for the deciduous forest obtained with the radial quantization strategy QS_{ρ} (selected on the validation set).

Tree	Classification Accuracy					
	Proposed Method			SoA Method		
	PA(%)	UA(%)	F1	PA(%)	UA(%)	F1
SB	93.3	93.3	0.93	57.1	53.3	0.55
RO	93.3	93.3	0.93	56.2	60.0	0.58
OA%	93.3			56.6		

TABLE VI: Classifications accuracies obtained on the test set for the conifer forest obtained with the hybrid quantization strategy $QS_{\alpha\rho}$ (selected on the validation set).

Tree	Classification Accuracy					
	Proposed Method			SoA Method		
	PA(%)	UA(%)	F1	PA(%)	UA(%)	F1
NS	86.0	86.0	0.86	66.6	66.6	0.66
EL	80.0	80.0	0.80	47.0	53.3	0.50
SP	93.0	93.0	0.93	50.0	46.6	0.48
SF	86.0	86.0	0.86	85.7	80.0	0.82
OA%	86.6			61.6		

TABLE VII: Classifications accuracies obtained on the test set for the mixed forest obtained with the hybrid quantization strategy $QS_{\alpha\rho}$ (selected on the validation set).

Tree	Classification Accuracy					
	Proposed Method			SoA Method		
	PA(%)	UA(%)	F1	PA(%)	UA(%)	F1
NS	87.2	93.5	0.90	50.0	46.6	0.48
EL	84.2	73.4	0.78	53.3	53.3	0.53
SP	58.5	66.1	0.62	46.6	46.6	0.46
SF	81.1	86.5	0.83	63.3	46.6	0.53
SB	75.2	60.0	0.66	50.0	66.6	0.57
RO	75.8	80.6	0.77	53.3	53.3	0.53
OA%	76.6			52.2		

IV. CONCLUSION

In this paper, a crown quantization based approach to tree species classification on high density ALS data is proposed. Unlike the standard approaches, rather than focusing the attention on specific crown features, the proposed approach proposes a data-driven quantization of 3D crown in order to capture the distinctive spatial and spectral crown characteristics of tree species. The individual tree crown span is approximated using a cylindrical parametric model. The

space enclosed by the cylinder is quantized into finer 3D elementary subvolumes, the ECVs, to perform a comprehensive analysis of the crown. For each tree, a histogram feature vector is obtained by progressively stacking the ECV feature sets derived from the point-data enclosed by the ECV. Three quantization strategies including the angular QS_α , the radial QS_ρ , and the hybrid $QS_{\alpha\rho}$ were tested and compared. For each classification problem, the best quantization strategy and parameters are automatically identified in the training phase without requiring prior knowledge on the type of forest.

In the experimental analysis, we compared the proposed method with a SoA method [1] presented in the literature which extensively analyzes the ALS features for tree species classification. By this comparison, we observed that the proposed approach significantly outperforms the standard method due to its enhanced ability to derive local crown characteristics over the SoA method. This condition allows the extraction of local information that leads to an accurate species classification. Moreover, the proposed method does not require any separate feature selection step due to the high generalization ability of SVMs with the histogram kernel.

As future development, we plan to test the proposed method on heterogeneous forests, considering different forest species and to analyze its effectiveness on full waveform LiDAR data.

ACKNOWLEDGMENT

The authors would like to thank the "Dipartimento Risorse Forestali e Montane" of the Autonomous Province of Trento for providing the high-density LiDAR data used in this study. The data were acquired in the framework of the FORLIDAR project.

REFERENCES

- [1] Y. Lin and J. Hyypää, "A comprehensive but efficient framework of proposing and validating feature parameters from airborne lidar data for tree species classification," *International journal of applied earth observation and geoinformation*, vol. 46, pp. 45–55, 2016.
- [2] M. Maltamo, E. Næsset, and J. Vauhkonen, "Forestry applications of airborne laser scanning," *Concepts and case studies. Manag For Ecosys*, vol. 27, p. 460, 2014.
- [3] C. Paris and L. Bruzzone, "A growth-model-driven technique for tree stem diameter estimation by using airborne lidar data," *IEEE Transactions on Geoscience and Remote Sensing*, vol. 57, no. 1, pp. 76–92, 2018.
- [4] J. Heinzl and B. Koch, "Investigating multiple data sources for tree species classification in temperate forest and use for single tree delineation," *International Journal of Applied Earth Observation and Geoinformation*, vol. 18, pp. 101–110, 2012.
- [5] K. Johansen and S. Phinn, "Mapping structural parameters and species composition of riparian vegetation using ikonos and landsat etm+ data in australian tropical savannahs," *Photogrammetric Engineering & Remote Sensing*, vol. 72, no. 1, pp. 71–80, 2006.
- [6] I. Chuine and E. G. Beaubien, "Phenology is a major determinant of tree species range," *Ecology Letters*, vol. 4, no. 5, pp. 500–510, 2001.
- [7] M. Torma, "Estimation of tree species proportions of forest stands using laser scanning," *International Archives of Photogrammetry and Remote Sensing*, vol. 33, no. B7/4; PART 7, pp. 1524–1531, 2000.
- [8] C. Paris, D. Valduga, and L. Bruzzone, "A hierarchical approach to three-dimensional segmentation of lidar data at single-tree level in a multilayered forest," *IEEE Transactions on Geoscience and Remote Sensing*, vol. 54, no. 7, pp. 4190–4203, 2016.
- [9] A. Persson, J. Holmgren, and U. Söderman, "Detecting and measuring individual trees using an airborne laser scanner," *Photogrammetric Engineering and Remote Sensing*, vol. 68, no. 9, pp. 925–932, 2002.
- [10] F. Morsdorf, E. Meier, B. Kötz, K. I. Itten, M. Dobbertin, and B. Allgöwer, "Lidar-based geometric reconstruction of boreal type forest stands at single tree level for forest and wildland fire management," *Remote Sensing of Environment*, vol. 92, no. 3, pp. 353–362, 2004.
- [11] J. Reitberger, C. Schnörr, P. Krzystek, and U. Stilla, "3d segmentation of single trees exploiting full waveform lidar data," *ISPRS Journal of Photogrammetry and Remote Sensing*, vol. 64, no. 6, pp. 561–574, 2009.
- [12] V. F. Strimbu and B. M. Strimbu, "A graph-based segmentation algorithm for tree crown extraction using airborne lidar data," *ISPRS Journal of Photogrammetry and Remote Sensing*, vol. 104, pp. 30–43, 2015.
- [13] A. Harikumar, F. Bovolo, and L. Bruzzone, "Subdominant tree detection in multi-layered forests by a local projection of airborne lidar data," in *Geoscience and Remote Sensing Symposium (IGARSS), 2017 IEEE International*. IEEE, 2017, pp. 2760–2763.
- [14] M. Dalponte, L. Bruzzone, and D. Gianelle, "Fusion of hyperspectral and lidar remote sensing data for classification of complex forest areas," *IEEE Transactions on Geoscience and Remote Sensing*, vol. 46, no. 5, pp. 1416–1427, 2008.
- [15] —, "Tree species classification in the southern alps based on the fusion of very high geometrical resolution multispectral/hyperspectral images and lidar data," *Remote sensing of environment*, vol. 123, pp. 258–270, 2012.
- [16] H. O. Ørka, E. Næsset, and O. M. Bollandsås, "Classifying species of individual trees by intensity and structure features derived from airborne laser scanner data," *Remote Sensing of Environment*, vol. 113, no. 6, pp. 1163–1174, 2009.
- [17] J. Holmgren and Å. Persson, "Identifying species of individual trees using airborne laser scanner," *Remote Sensing of Environment*, vol. 90, no. 4, pp. 415–423, 2004.
- [18] J. Vauhkonen, T. Tokola, P. Packalén, and M. Maltamo, "Identification of scandinavian commercial species of individual trees from airborne laser scanning data using alpha shape metrics," *Forest Science*, vol. 55, no. 1, pp. 37–47, 2009.
- [19] C. Ko, G. Sohn, and T. K. Rimmel, "Tree genera classification with geometric features from high-density airborne lidar," *Canadian Journal of Remote Sensing*, vol. 39, no. sup1, pp. S73–S85, 2013.
- [20] A. Harikumar, F. Bovolo, and L. Bruzzone, "An internal crown geometric model for conifer species classification with high-density lidar data," *IEEE Transactions on Geoscience and Remote Sensing*, vol. 55, no. 5, pp. 2924–2940, 2017.
- [21] Å. Persson, J. Holmgren, U. Söderman, and H. Olsson, "Tree species classification of individual trees in sweden by combining high resolution laser data with high resolution near-infrared digital images," *International Archives of Photogrammetry, Remote Sensing and Spatial Information Sciences*, vol. 36, no. 8, pp. 204–207, 2004.
- [22] X. Yu, P. Litkey, J. Hyypää, M. Holopainen, and M. Vastaranta, "Assessment of low density full-waveform airborne laser scanning for individual tree detection and tree species classification," *Forests*, vol. 5, no. 5, pp. 1011–1031, 2014.
- [23] H. Ørka, E. Næsset, and O. Bollandsås, "Utilizing airborne laser intensity for tree species classification," *International Archives of the Photogrammetry, Remote Sensing and Spatial Information Sciences*, vol. 36, no. Part 3, p. W52, 2007.
- [24] R. Blomley, A. Hovi, M. Weinmann, S. Hinz, I. Korpela, and B. Jutzi, "Tree species classification using within crown localization of waveform lidar attributes," *ISPRS Journal of Photogrammetry and Remote Sensing*, vol. 133, pp. 142–156, 2017.
- [25] P. Thomas, *Trees: their natural history*. Cambridge University Press, 2014.
- [26] K. Wang, T. Wang, and X. Liu, "A review: Individual tree species classification using integrated airborne lidar and optical imagery with a focus on the urban environment," *Forests*, vol. 10, no. 1, p. 1, 2019.
- [27] A. Barla, F. Odone, and A. Verri, "Histogram intersection kernel for image classification," in *Proceedings 2003 International Conference on Image Processing (Cat. No.03CH37429)*, vol. 3, Sept 2003, pp. III–513.
- [28] D. Gatzliolis, "Dynamic range-based intensity normalization for airborne, discrete return lidar data of forest canopies," *Photogrammetric Engineering & Remote Sensing*, vol. 77, no. 3, pp. 251–259, 2011.